Soft Matter

Photo-responsive liposomes composed of spiropyran-containing triazole-phosphotidylcholine: Investigation of merocyanine-stacking effects on liposome-fiber assemly-transition

Journal:	*Soft Matter*
Manuscript ID	SM-ART-10-2018-002181.R2
Article Type:	Paper
Date Submitted by the Author:	26-Mar-2019
Complete List of Authors:	Zhang, Dawei; University of Colorado, Department of Chemical and Biological Engineering Shah, Parag; University of Colorado Boulder Culver, Heidi; University of Colorado at Boulder, Chemical and Biological Engineering David, Sabrina; University of Colorado Boulder, Material Science and Engineering Program Stansbury, Jeffrey; University of Colorado, Department of Chemical and Biological Engineering Yin, Xiaobo; University of Colorado Boulder, Mechanical Engineering Bowman, Christopher; University of Colorado, Department of Chemical and Biological Engineering

Journal Name

ARTICLE

Photo-responsive liposomes composed of spiropyran-containing triazole-phosphotidylcholine: Investigation of merocyanine-stacking effects on liposome-fiber assemly-transition

Received 00th January 20xx,
Accepted 00th January 20xx

DOI: 10.1039/x0xx00000x

www.rsc.org/

Dawei Zhang[a,c], Parag K. Shah[a], Heidi R. Culver[a], Sabrina N. David[c], Jeffrey W. Stansbury[a,c], Xiaobo Yin[b,c] and Christopher N. Bowman*[a,c]

A spiropyran-containing triazole-phosphotidylcholine (SPTPC) was synthesized through a copper-catalyzed azide alkyne cyclo-addition (CuAAC) reaction. In water, SPTPCsself-assembled and a spontaneous spiropyran-to-merocyanine (SP-to-MC) isomerization occurred, resulting in coexistence of liposomes and fibers, and switchingfrom the spiropyran (SP) to the merocyanine (MC) isomeric structure induced a reversible transition between these molecular assemblies. Study of the self-assembly of SPTPCs and photo-induced liposome-fiber assembly-transition revealed that the presence of MC enabled additional inter-membrane interaction during self-assembly and that MC-stacking effect was the driving force for the assembly-transition. Exposure to UV light induced switching from SP to MC, where the planar structure of MC and the confinement of MC led to enhanced MC-stacking. The effect of MC-stacking was both advantageous and disadvantageous: MC-stacking perturbed the hydrophobic phase in the bilayer membrane and facilitated the liposome-to-fiber transition, otherwise the MC-stacking retarded swtiching of MC to SP, and caused an incomplete recovery of MC to SP during fiber-to-liposome recovery, thus a fatigue of SP was induced by the MC-stacking during theliposome-to-fiber transition cycle. To decrease the intermolecular interactions and suppress MC-stacking, photo-inert triazole-phosphotidylcholine (TPC) was incorporated to prepare two-component TPC/SPTPC-liposomes, which exhibited better recovery kinetics. The photo-adaptive behavior of TPC/SPTPC-liposomes confirmed the disturbance of bilayer membranes by inter-membrane MC-stacking and the formation of MCTPC-enriched phases in the bilayer membrane.

Introduction

Self-assembly of amphiphilic molecules into supramolecular structures is a common phenomenon in nature. Non-covalent interactions among molecules, including hydrophobic effects, electrostatic interactions, hydrogen bonding, π-π stacking, metal-ligand coordination, and host-guest complex, are all potential driving forces to be used for self-assembly.[1-6] Although non-covalent interactions are not as robust as covalent bonding, their intrinsic dynamic character leads to assemblies with adaptivity, where the structure or properties of the supramolecular assemblies change in response to a surrounding perturbation.[7]Different amphiphiles have distinct responsiveness to certain stimuli (e.g., ionic strength, pH value, temperature etc.). The stimuli-responsiveness is a result of thermodynamic equilibrium and alters assembly properties including molecular interactions, phase transitions, permeability, and overall morphology.[8-13]

From the viewpoint of materials science, assemblies with stimuli responsive morphological changes are of special interest. Stimuli-responsive self-assembly usually follows a "small perturbation, large response"model,[14]allowing morphology and other properties to be precisely controlled using external triggers. Thus, the macroscopic properties of the assemblies are dynamically controlled by adjusting the degree of perturbation, which makes the responsive assemblies promising candidates for smart materials. Some examples include pH-dependent visco-elasticity of peptide supramolecular hydrogels;[15] ionic strength dependent dissociation of nucleolipid organogels;[16] photo-controlled permeability of polyersomes;[17] photo/pH dual controlled fluorescence emission of micelles,[18]and light-induced assembly-transitions (e.g., tubular to vesicle or micelle to fiber).[19] These functional assemblies and corresponding stimuli-responsive adaptivity have potential biological applications, such as for injectable implants,[20, 21] controlled release,[22, 23] bio-imaging, and bio-detection.[24-27] Furthermore, in the emerging research field of artificial cells, stimuli-adaptive assemblies are promising candidates for construction of cell-like units.[28] In some cases, studying the stimuli-adaptivity of assemblies at the molecular and meso-phase scales may lead to a better understanding of cell behavior and life activities.[29, 30] Among stimuli-adaptive assemblies, photo-responsive liposomes are of special interest due to their resemblance to cells (i.e., phospholipid composition, bilayer membrane structure, and

[a] Department of Chemical and Biological Engineering, University of Colorado Boulder, UCB 596, Colorado 80309, United States.
[b] Department of Mechanical Engineering, University of Colorado, Boulder, CO 80309, USA
[c] Materials Science and Engineering Program, University of Colorado, Boulder, CO 80309, USA
Electronic Supplementary Information (ESI) available: See DOI: 10.1039/x0xx00000x

vesicular contour) and the ability to non-destructively trigger the response using light, with excellent spatial and temporal control.

Here, we report the study of photo-responsive liposomes composed of spiropyran-containing triazole-phosphotidylcholines (SPTPC). Upon application and subsequent cessation of UV-irradiation, the switch between spiropyran (SP) and merocyanine (MC) groups leads to a reversible transition between liposome and fibrous assemblies. Spectroscopic and microscopic studies revealed that the inter-molecular interactions among MCs, especially the MC-stacking effect, trigger the assembly-transition. This SP-based dynamic liposomal assembly provides a tool to construct artificial cells with photo-adaptive morphologies and is a candidate for potential biological applications.

Experimental

Synthesis of alkyne lysolipid (AL), spiropyran-containing azide precursor (SPN_3) and spiropyran-containing triazole-phosphotidylcholine (SPTPC)

Please see electronic supplementary information for a description of synthesis (ESI, 2.1 Synthesis of spiropyran-containing azide precursor. 2.2 Synthesis of alkyne lysolipid).

Preparation of SPTPC-liposomes (*in-situ*method and hydration method)

In the *in-situ* method, alkyne phospholipid (AL) (1 eq) and spiropyran-containing azideTN_3 (1 eq) precursors were dispersed in water (pH=7.04) to obtain a 1mM precursor dispersion (with or without 0.005 mM rhodamine B 1,2-Dihexadecanoyl-sn-Glycero-3-Phosphoethanolamine triethylammonium salt (R-DHPE) as the fluorescent dye). Concentrated aqueous solutions of $CuSO_4$ (0.05 eq) and sodium ascorbate (0.1 eq) were added subsequently to catalyze the copper-catalyzedazide alkyne cyclo-addition (CuAAC) reaction. The mixture was then incubated at room temperature for 12 h.

In the hydration method, chloroform was evaporated from the SPTPC solution under vaccum to obtain a SPTPC solid film (0.496 mg, 0.0004 mmol), (with or without 0.005 mM R-DHPE as the fluorescent dye). Water (0.4 mL, pH=7.04) was added to hydrate the SPTPC film for 12 h.

Accordingly, the SPTPC/triazole-phosphotidylcholine (TPC)-liposome samples were prepared using thehydration method with different molar percentages of SPTPC and TPC, keeping the concentration of SPTPC constant at 1 mM (or 10 mM).

For preparation of uni-lamellar liposome with controlled diameter, a tip-sonicator and a membrane extruder were used. The hydrated phospholipid was vortexed for 5 minutes, and was sonicated for 5 minutes in pulse model, with controlled output power. Finally the turbid dispersion was extruded through polycarbonate membrane with 100 nm pore size 15 times.

Cryo-TEM imaging

Three 2µL-liposomes samples were dropped on carbon-coated copper grids, separately. The first sample was directly frozen using an FEI Vitrobot Mark IV manual plunge freeze device. The other two samples were irradiated with 365 nm light (15 mW/cm^2), and one of the twoexposed samples was frozen immediately after UV-exposure. The last sample was left to recover for 2 h prior to freezing. Imaging of the liposome samples was performed using an FEI Tecnai F30FEG-TEM operating at 300 kV.

Wide-angle X-ray scattering (WAXS) measurement

WAXSexperiments were conducted atroom temperature (20 ℃). The sample concentration was 10 mM SPTPC. Acapillary with 10 µm wall-thickness was employedto load samples, and the optical path was 1 mm. A 30 W Genix 3D X-ray generator(Cu anode, wavelength = 1.54 angstrom) was used and a beam of size 0.8 × 0.8 mm^2 was applied onall samples, (~4 × 10^7 photons/s flux was achieved in the beam). A DectrisEiger R 1M detector was used for data collection. X-ray passed through a vacuum pipe of 120 cm. The distance between the sample and outlet of the vacuum pipe was 4 cm, and the sample-to-detector distance was 16 cm. The flight-path of scattered X-ray was in air.

Dynamic light scattering (DLS) measurement

Measurements were performed using a Zetasizer Nano ZSP instrument (Malvern) using disposablepolystyrenecuvettes. The temperature was set at 25 ℃, the measurement angle was 173 degree (default). The mean hydrodynamic diameter of the

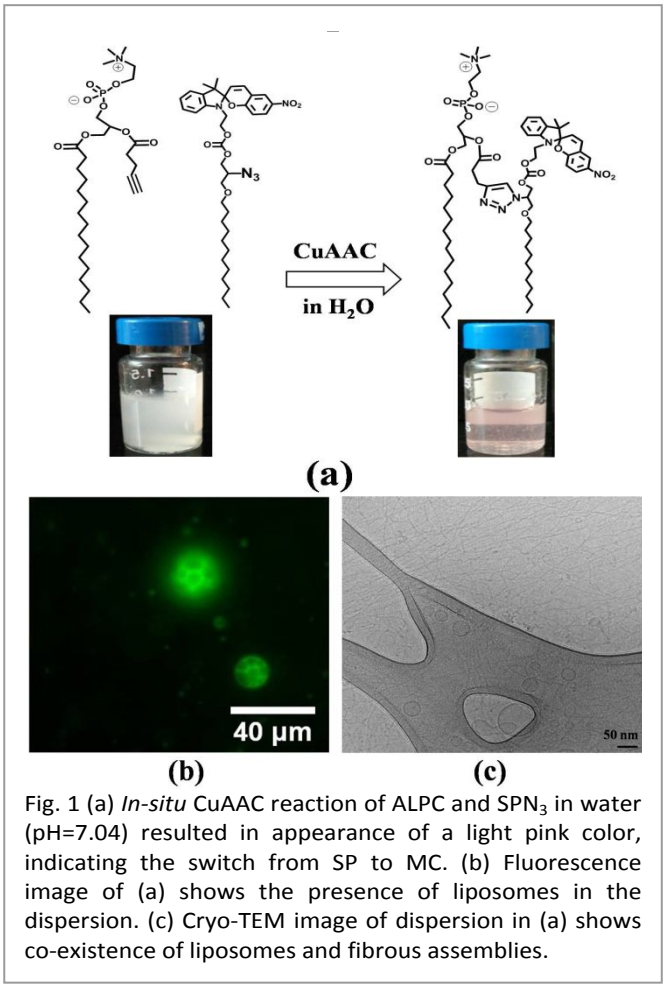

Fig. 1 (a) *In-situ* CuAAC reaction of ALPC and SPN_3 in water (pH=7.04) resulted in appearance of a light pink color, indicating the switch from SP to MC. (b) Fluorescence image of (a) shows the presence of liposomes in the dispersion. (c) Cryo-TEM image of dispersion in (a) shows co-existence of liposomes and fibrous assemblies.

liposomes (D_h) was computed from the intensity of the scattered light using the Malvern software package based on the theory of Brownian motion and the Stokes–Einstein equation. Instrument parameters were kept the same for measurements after 365 nm UV irradiation, sample was irradiated by 365 nm LED light (15 mW/cm^2, 2 minutes).

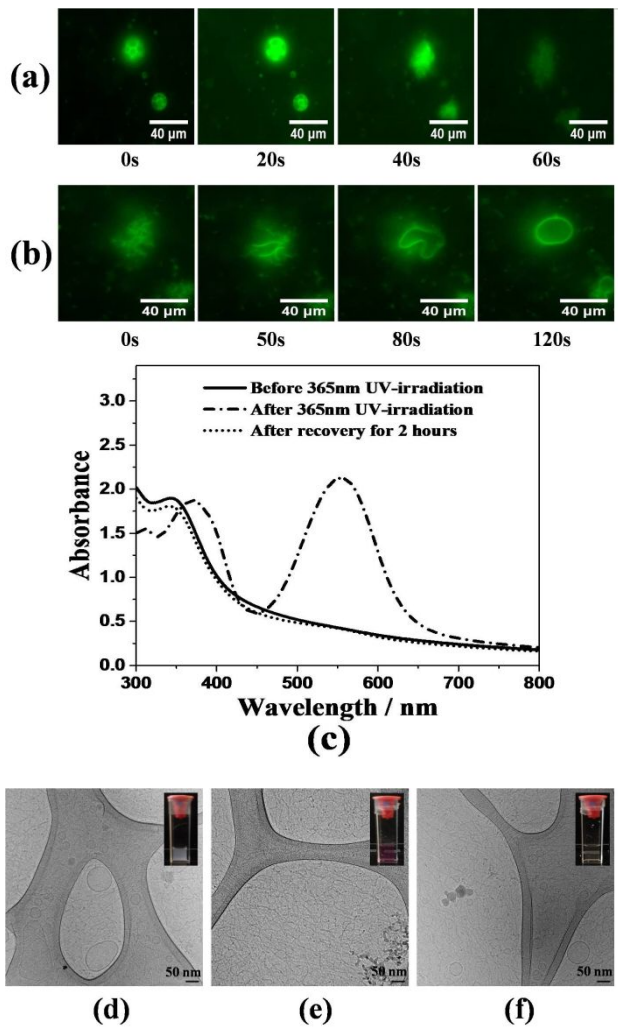

Fig. 2 (a) Fluorescence microscopy images showing the photo-induced morphological changes of SPTPC-liposomes upon exposure to 365nmlight (15 mW/cm^2, 1 minute). (b) Recovery of liposomal contour after removal of 365nm light. (c) UV-vis spectra show the change of absorption bands of SPTPC during one irradiation-recovery cycle, and verify that the SP←→MC transition induced the morphological change, solid line---before UV-irradiation; dot dash line---after UV-irradiation; dash line---recovered spectra following two hours in the dark.Cryo-TEM images of liposome samples. (d) before and (e) after 365nm UV-irradiation, and (f) after two-hours of recovery in the dark, illustrate the assembly-transition between liposomes and fibers. Insets in images show the changes in appearance of the sample corresponding to the different treatments. SPTPC-liposomes were prepared by *in-situ*CuAAC reactions in water (pH=7.04).

UV-vis spectra

SPTPCs were dissolved in different organic solvents, and SPTPC-liposomes and SPTPC/TPC-liposomes were prepared using the hydration method. The concentration of total phospholipid concentration in each sample was maintained at 1 mM or 10 mM. Samples were transferred into a 5 mm×5 mm quartz-cuvette. Spectra were recorded in the range of 300-800 nm in absorbance mode with a bandwidth of 2 nm and a scanning speed of 600 nm/min.

For monitoring the recovery kinetics, liposome-samples were irradiated for 2 min (15 mW/cm^2) before continuous spectral recording for 2 h.

Light microscope imaging

Fluorescence images were recorded on a Zeiss Axiovert 200m Wide-field inverted microscope equipped with an EMCCD Camera. R-DHPE (0.005 mM)was used as the fluorescent dye and a 365 nm LED was used as the UV-light source.

The optical birefringence of bilayer membranes was observed using an Olympus (BX-51) optical microscope equipped with crossed polarizer and analyzer, and a full wavelength (530 nm) retardation wave-plate. Samples were irradiated from above using a 365 nm LED (15 mW/cm^2).

A fluorescence microscope with a photo-patterning setting was used for selective UV-exposure area (ESI, Fig S1). In this case, a 377 nm laser (operating at 8 mW output power) was applied as the UV-light source. Fluorescence microscopy images were recorded by a Nikon 5300 camera.

Results and discussion

***In-situ* formation of SPTPC-liposomes and reversible photo-induced morphological responsiveness.**

To confirm SPTPC-liposomeformation, coupling of AL and spiropyran-containing azide (SPN_3) precursors was performed directly in water (pH=7.04) through the CuAAC reaction (Fig. 1a). The reaction went to completion and the target SPTPC molecules were obtained as confirmed by ^{1}H NMR (ESI, NMR spectra section). Self-assembly occurred immediately after the formation of SPTPC molecules, as evidenced by the liposomes observed via fluorescence microscopy (Fig. 1b). The generation of SPTPC-liposomes resulted in the visual appearance of color (Fig. 1a, inset), which indicated a switch from the colorless SP form to the colored MC form.[31] It was hypothesized that the SP-to-MC switch was induced because SP was confined at the hydrophilic-hydrophobic interface. Specifically, it is known that SP exhibits solvatochromism, where interactions with water molecules stabilize the MC form relative to the SP form. Furthermore, Cryo-TEM imaging showed the co-existence of liposomes and fibrous assemblies (Fig. 1c). The formation of fibrous assemblies is likely caused by merocyanine triazole-phosphotidylcholine (MCTPC), the ring-opened, zwitterionic form of SPTPC.[32] The presence of both assembly types

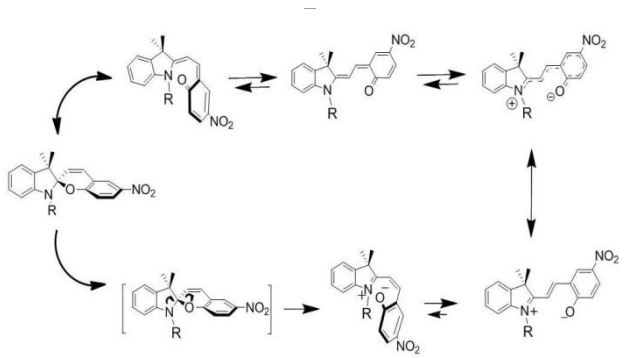

Scheme 1 Switch pathway between spiropyran and merocyanine.

suggested that switching between SPTPC and MCTPCcouldinduce a reversible assembly-transition between liposomes and fibers.

To investigate the morphological change of SPTPC-liposomes upon photo-switching of SP to MC, a time-lapse fluorescence microscopy experiment was performed. Fig. 2a showed that upon 365 nm UV-irradiation, the vesicular contour of the observed SPTPC-liposomes gradually deformed and became ambiguous, and the fluorescent signal grew dim. Interestingly, after cessation of UV irradiation, liposome re-organization was observed (Fig. 2b). Correspondingly, absorption spectra before and after 365 nm UV-irradiation were recorded (Fig. 2c). Switching from the SP form to the MC form resulted in emergence of an MC absorbance peak around 543 nm. After removal of UV-light, the intensity of the MC peak decayed and almost disappeared after two hours in the absence of light, which verified the spontaneous thermal recovery of MC to SP. The cryo-TEM images of the samples before and after UV-irradiation confirmed the photo-induced, reversible assembly-transition between liposomes and fibers (Fig. 2d, 2e, 2f). In the control group, liposomes composed of TPC without covalently bonded spiropyran groups were formed through *in-situ* CuAAC coupling of AL and aliphatic azide. ThecontrolTPC-liposomesshowed no morphological changes during 365 nm UV-irradiation (ESI, movie S1), further confirming the hypothesis that the SP-MC switch was responsible for the transition between assemblies. For liposomes prepared by CuAAC-driven *in-situ* formation, residual catalyst (i.e., Cu (I) and Cu (II)) can interact with the zwitterionic merocyanine, and cause unexpected sample changes, such as the turbidity decrease observed after irradiation (Fig. 2d, 2e, 2f). Thus, in the remaining studies, assembly of SPTPC in water was obtained by the hydration method.

Study of SPTPC assembly

Spiropyran is an intensively studied photochrome, and the switching pathway between spiropyran (SP) and merocyanine (MC) has been presented previously (Scheme 1).[33] Specifically, the MC form is a resonance hybrid between zwitterionic and neutral quinoidal isomers. The dominant isomer varies depending on the specific environmental conditions and can be characterized by the absorptionspectra. In the SPTPC molecule, the SP group is chemically bonded with the PC moiety and can approach the hydropholic choline head, or the hydrophobic aliphatic chains. Due to the special position of SP in the SPTPC structure, when SPTPCs self-assemble in water, isomerisation of SP will be influenced by both polar and non-polar micro-environments. Thus, in the SPTPC assembly, SP groups may reside in environments with different polarities and exhibit distinctive isomeric forms. A study of the isomeric forms of SP groups could provide insight into the influence of isomerization on assembly behaviour and, specifically, help to understand the liposome-fiber assembly-transition.

SPTPC assemblies were prepared by the hydration method, rather than the CuAAC-driven *in situ* method, in order to prohibit formation of the metal-MC complex upon UV-irradiation and the corresponding influence of the metal-MC complex on the maximum absorption position (λ_{max}) of monomeric MC.[34, 35]

A dry SPTPC film on a quartz plate was colorless, and exhibited a typical absorption spectrum of SP (Fig. 3a, 3b). WAXS revealed that in the dry film there were periodic structures (Fig. 3c). Specifically, a sharp Bragg reflection band centered at Q=0.156 $Å^{-1}$ was ascribed to lamellar periodic structure with an inter-lamellar spacing (d) around 4 nm (first order diffraction), and the multi-peak character of the band of the lamellar structure (Q=0.156 $Å^{-1}$) indicated a variation of thickness of the lamellar structure, which was likely caused by interdigitation of the aliphatic chains during drying of organic solvent (Fig. 3c inset). A smaller reflection at Q=0.287 $Å^{-1}$ was ascribed to second harmonics of the first order diffraction.[36, 37] A broad peak at Q=1.400 $Å^{-1}$ reflected the spacing between the aligned aliphatic chains in the lamellar bilayer-membrane.[38] After hydration for 24 hours by immersion in water (pH=7.04), the hydrated SPTPC film showed a characteristic red colour of the MC form (Fig. 3d), and the presence of MC was confirmed by emergence of an MC-peak (540 nm) in the absorption spectrum (Fig. 3e). In 1-D WAXS curve of the hydrated SPTPC film, the diffraction peaks at Q=0.156 $Å^{-1}$ and Q=0.287 $Å^{-1}$ were attenuated (Fig. 3f). The peak-broadening was induced by penetration of water molecules to the inter-lamellar spaces, leading to hydration of the choline headgroups and disturbance of the stacking lamellar structure. Penetration of water molecules caused different layer spacing and resulted in hydrated multi-lamellar structures with disordered stacking. The stacking disorder wasreflected by diffraction peaks at Q=0.08, 0.12, and 0.16$Å^{-1}$ (Fig. 3f inset). A broad diffraction peak at Q=1.4 $Å^{-1}$ further confirmed the presence of bilayer structures (Fig. 3f). Specifically, the 1-D WAXS curvesof dry and hydrated SPTPC films both exhibited a typical profile of a bilayer structure: two broad bandscentered at Q=0.19$Å^{-1}$ (3.3 nm) and Q=0.4$Å^{-1}$ (1.6 nm).[39] The absorption spectra and WAXS results suggested that the hydration of choline headgroups created a polar micro-environment in which a solvent-induced SP-to-MC switchoccurred, because MC is the thermodynamically favoured form in polar conditions.[40] Meanwhile, the aliphatic chains of SPTPC formed a non-polar micro-environment in which SPs could retain ring-closed form, as Fig. 3g shows. It

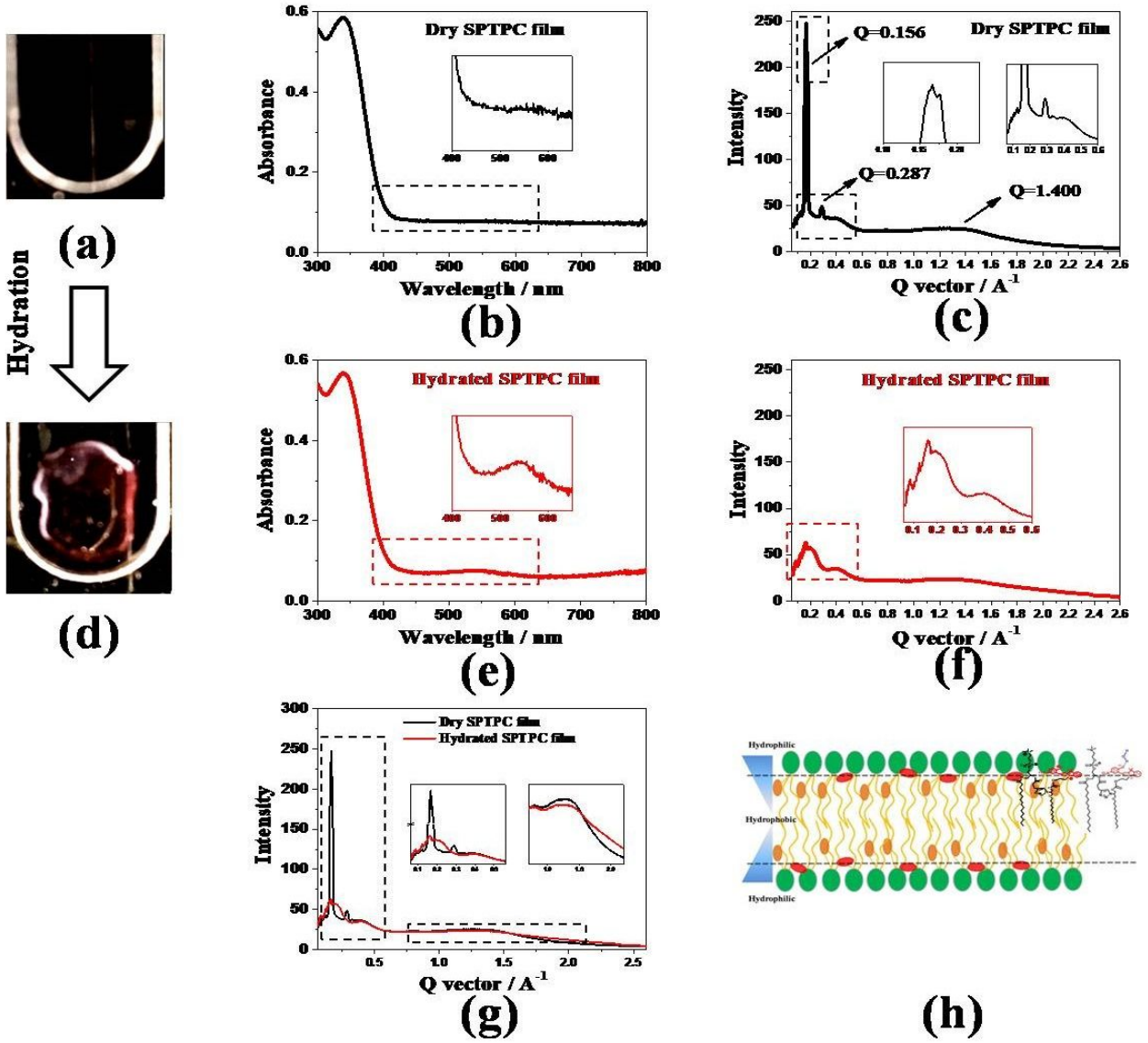

Fig. 3 (a) Dry SPTPC film on quartz plate. (b) Absorption spectra of the dry SPTPC film. (c) 1-D WAXS curve of dry SPTPC film reveals presence of periodic structures before hydration. (d) Hydrated SPTPC film shows a red color, indicating SP-to-MC switch. (e) Absorption spectra of hydrated SPTPC film. Appearance of MC peak confirms a porton SPs were switched to MC isomer. (f) 1-D WAXS curve of hydrated SPTPC film shows change of periodic structure which was caused by hydration of choline head of SPTPC. (g) Overlapping of 1-D WAXS curves of SPTPC film before and after hydration. (h) Illustrative figure of SPTPC bilayer membrane depicts a water-induced SP-to-MC switch at the hydrophilic/hydrophobic interface, and the polarity-gradient across the interface. Red ellipse—merocyanine; orange ellipse—spiropyran.

should be noted that though the SPTPCs assembled and formed bilayer structures after hydration, the hydrated SPTPC film was not easily dispersed in water by gentle vibration, which may be attributed to the presence of zwitterionic MCs leading to inter-lamellar interactions.

The hydrated SPTPC film could be further dispersed in water by mechanical vibration (i.e., vortex), but resulted in some flocculation. Dispersion of SPTPC assemblies caused a stronger MC-absorption due to increased interactions with water molecules (Fig. 4a black curve). The MC-absorption spectrum showed two overlapping bands (Fig. 4b), with the λ_{max} of the two peaks located at 543 nm and 567 nm, respectively. In polar solvents, SP underwent a spontaneous switch to MC, and λ_{max} of the MC band depends on the solvent polarity.[32] Thus, the two overlapping MC bands suggested that in the SPTPC bilayer membrane, a polarity-induced SP-to-MC switch occurred and the formed MC was located in micro-environments of different polarity. Specifically, MC was likely localized across the hydrophilic/hydrophobic interface of the bilayer membrane (i.e., across a polarity gradient). The λ_{max} of the two MC peaks were in accordance with that of SPTPC in methanol solution (543 nm) and SPTPC DMSO solution (567 nm) (ESI, Fig. S2).

To obtain well dispersed SPTPC assemblies, a tip sonicator and a membrane extruder were applied to the dispersion.

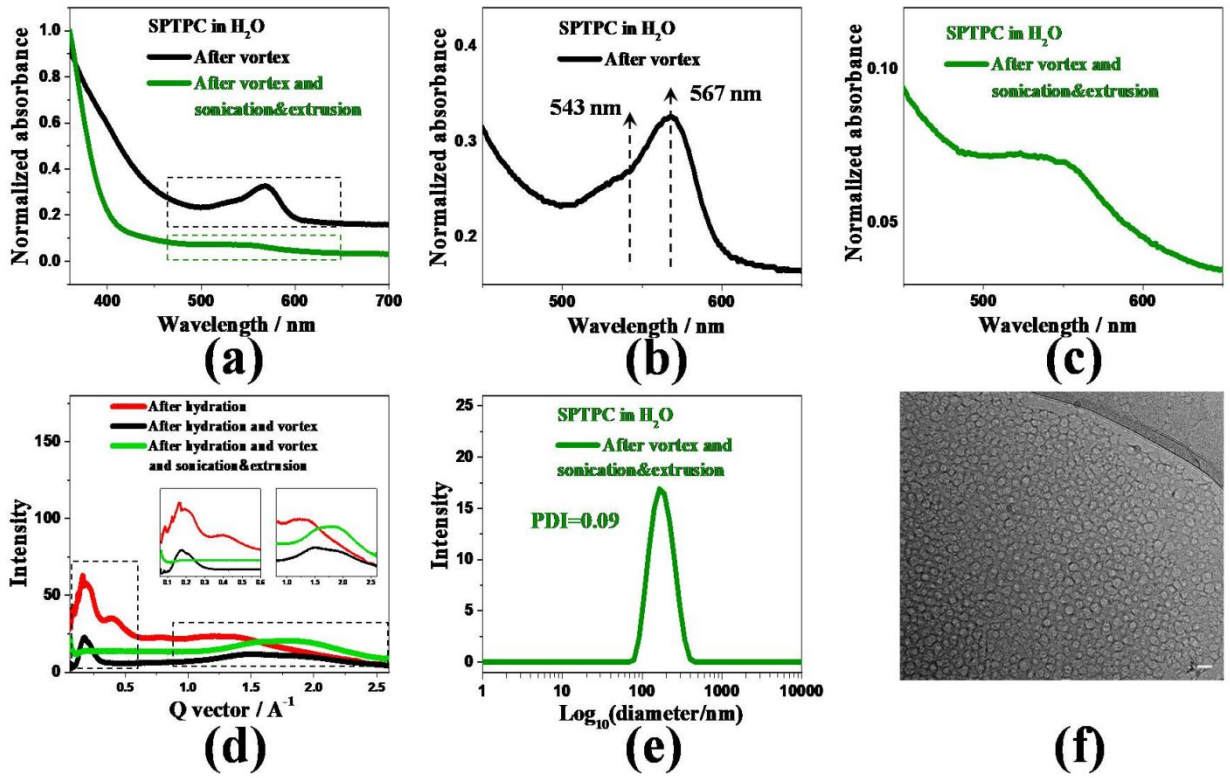

Fig. 4 (a) Absorption spectra of SPTPC liposomes (black----after vortex; green----after vortex and sonication&extrusion). (b) Expanded spectra of SPTPC-liposomes after vortexing. The overlapped MC bands indicate MCs locate across the hydrophilic/hydrophobic interface of the bilayer membrane where polarity-gradients exist. (c) Expanded spectra of SPTPC-liposome after sonication&extrusion. Attenuation of MC absorption verifies a MC-to-SP recovery after sonication&extrusion. (d) 1-D WAXS curve of SPTPC samples in H_2O (red----hydrated SPTPC film; black----after vortex of hydrated SPTPC film; green----after vortex and sonication&extrusion of SPTPC film). (e) Size distribution curve of SPTPC in H_2O (after vortex and sonication&extrusion). After sonication and extrusion, liposomes with low polydispersity were prepared. (f) Cryo-TEM image of SPTPC-liposomes prepared by hydration, vortex and sonication&extrusion, scale bar = 100 nm. The concentration of SPTPC was 10mM.

Sonication and membrane extrusion are usually applied to prepare uni-lamellar liposomes with narrow size distribution. Figure 4a-c shows the effects ofsonication and extrusion on the absorption spectra of SPTPC assemblies. Compared to absorption spectra before sonication&extrusion (Fig. 4a black curve, 4b), the MC peaks were attenuated after sonication and extrusion (Fig. 4a green curve, 4c). This attenuation indicated MC-to-SP recovery which is likely attributed to conversion of SPTPC multi-lamellar structure to uni-lamellar structures. WAXS assisted to illustrate the change of periodic structure during vortexing and subsequent sonication and extrusion (Fig. 4d). After vortexing, the lack of the sharp Bragg reflection (Q=0.08, 0.12 and 0.16 A^{-1} in Fig. 4d, red curve) confirmed disappearance of the stacking disorder ofthe multi-lamellar structure (Fig. 4d, black curve), and disappearance of the sub-diffraction band at Q=0.4 A^{-1}verified the decrease of the multi-lamellar structure. The main diffraction band at Q=0.19 A^{-1} was from the dispersed lamellar bilayers after vortex. After sonication and extrusion, the main diffraction was the disappearance of the band at 0.19 A-1, which likely results from dispersed bilayers in the form of spherical liposomes (Fig. 4d, green curve).[41]Formation of spherical liposomes was verified by cryo-TEM (Fig. 4f), and the size distribution curve from DLS showed that the SPTPC-liposome had a lower value of polydispersity.

The change of absorption spectra and 1-D WAXS curves of SPTPC film (hydrated, after vortex, after vortex and sonication and extrusion)indicate that the solvent-induced SP-to-MC switch could be enhanced by multi-lamellar structures, and indicated that the presence of MCs might induce an inter-membrane interaction.

Investigation of the photo-induced assembly-transition: stacking effect of MCs and phase-transition in bilayer membrane upon 365 nm UV irradiation

To investigate the role of MC group in liposome-to-fiber assembly-transition, spectroscopic properties of SP and MC were characterized during 365 nm UV-irradiation.

Upon 365 nm UV-irradiation, SPTPC in different solvents was switched to ring-opened MC form, as evidenced by emergence of an absorptionbandin the visible-light region with different λ_{max} depending on solvent polarity (Fig. 5a and Table

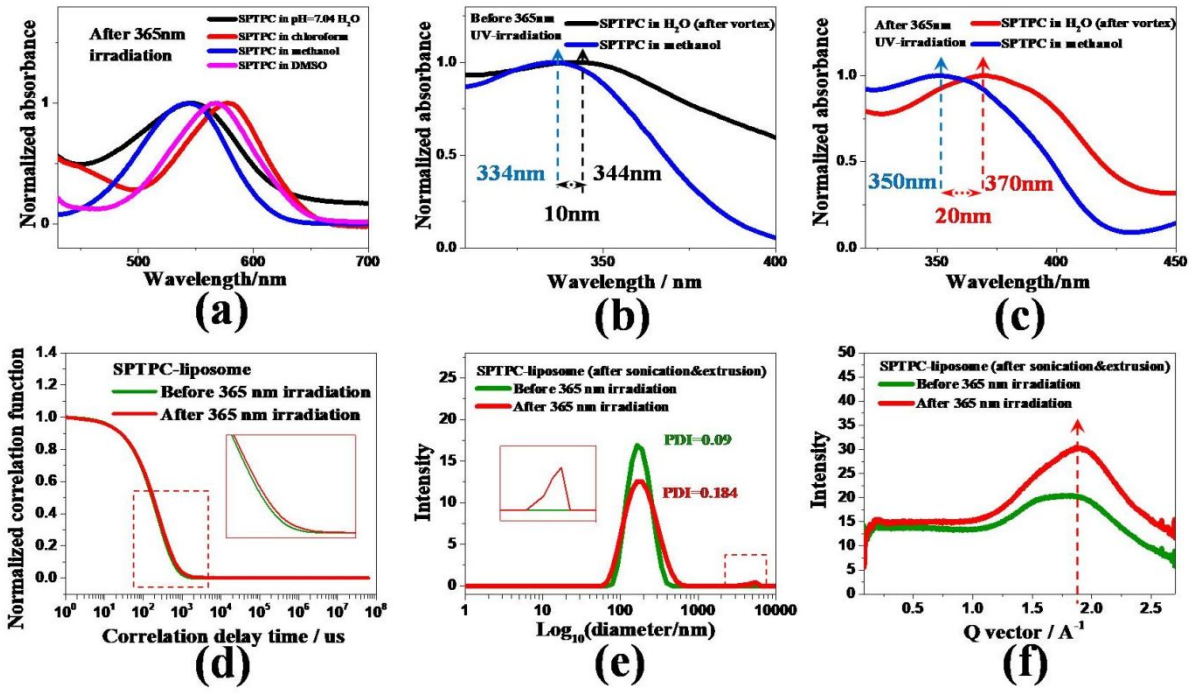

Fig. 5 (a) After 365 nm UV-irradiation, MC absorption bands of SPTPC-liposomes (only vortexed) and organic solutions of SPTPC exhibit different position of λ_{max}, which was induced by different polarity of solvents. (b) Before 365 nm UV-irradiation, absorption bands of the internal charge-transfer transition of SPTPC methanol-solution compared to SPTPC-liposomes (only vortexed). The difference in λ_{max} (10 nm) indicates J-type stacking in the bilayer membrane. (c) After 365 nm UV-irradiation, change of absorption bands of samples in (e). The enlarged difference of λ_{max} (from 10 nm to 20 nm) is caused by more red-shifting of absorption band of SPTPC-liposome (only vortexed), which verifies that the stacking effect was enhanced in the bilayer membrane. (d) Normalized correlation function decaying curve of SPTPC liposomes (sonicated&extruded) before and after 365 nm UV irradiation. Longer decaying time after irradiation was due to slower diffusion rate of fibrous assembly, which was formed in the photo-induced liposome-to-fiber transition. (e) Size distribution curve of SPTPC liposome (sonicated&extruded) before and after 365 nm UV irradiation. Broadening of peak and appearance of new peak verifies change of colloidal property during irradiation. (f) 1-D WAXS curve of SPTPC liposome (sonicated&extruded) before and after 365 nm UV irradiation. The concentration of SPTPC was 10 mM

1).Increased media polarity improved the stability (i.e., lowers the energy level of zwitterionic MC), resulting in a bathochromic shift of λ_{max} with increased solvent polarity. Previous research revealed that the monomeric zwitterionic MC is the dominant form in methanol.[42] The λ_{max} of the MCTPC aqueous sample has the same λ_{max} asMCTPC in methanol, suggesting that, under 365 nm UV-irradiation, the monomeric zwitterion-MC form was the dominant isomer in the bilayer membrane of SPTPC-liposomes.

Themonomericzwitterionic MCs provided additional molecular interactions in the bilayer membrane of liposomes, including electrostatic forces, hydrophilic affinity, and dipolar interactions, all of which perturbed the structural integrity of the bilayer membrane. In particular, the planar structure of MC could strengthen molecular stacking. SPs (or MCs) were confined at the hydrophobic/hydrophilic interface of the bilayer membranes, and corresponding crowded effect which could enhance the stacking of planar MC.

The stacking effect among MCs was confirmed by comparison of absorption spectra between SPTPC methanol solution and vortexed SPTPC-assembly dispersion. Before UV-irradiation, the absorption band of SPTPC in methanol had a λ_{max} at 334 nm (Fig. 5b), which corresponds to the internal charge-transfer transition of SP system.[43, 44] However, for SPTPC-liposomes, the λ_{max} ofthis absorption band was at 344 nm. The 10 nm-difference in λ_{max} suggested formation of J-type stacking of SPs in bilayer membrane, where the chromophores stack in a head-to-tail way.[45]This stacking effect of SPs before UV-exposure was probably due to the crowded SPs at the interface of the bilayer

Table 1 λ_{max} of absorption bands of SP in different solvents before and after 365 nm UV-irradiation

	Visible-light region				UV-light region		
	[a]$CHCl_3$	[a]MeOH	[a]DMSO	[b]H_2O	[a]MeOH	[b]H_2O	Δλ
Before UV	----	543	567	543,567	334	344	10
After UV	578	543	567	543	350	370	20

[a] SPTPC organic solution.

[b] SPTPC-liposomes sample.

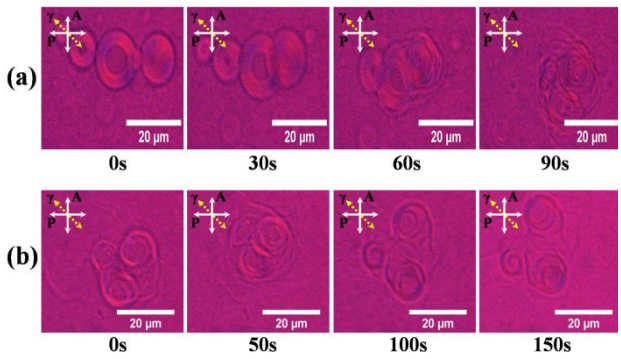

Fig. 6 Polarized optical microscopy (POM) images of liposomes (365 nm, 15 mW/cm^2), P: polarizer, A: analyzer, γ: a full wavelength (530 nm) retardation wave-plate with the slow axis marked with a yellow dashed arrow. (a) Under 365 nm UV-exposure, images show a gradual disappearance of birefringence of the bilayer membranes, confirming the perturbation of aligned hydrocarbon chains and the correspondent liquid crystal phase in the bilayer structure. (b) After removal of 365 nm UV-light, images show recovery of the interference colours, indicating re-alignment of hydrocarbon chains in the bilayer membrane and reformation of the liquid phase. Coincident with the change of interference colours is the morphological alternation during SP←→MC transition.

membrane. Upon 365 nm UV-irradiation, the λ_{max} of the absorption band had a red-shift to longer wavelengths for both two samples (350 nm in methanol and 370 nm in water) (Table 1, Fig. 5c). The enlarged λ_{max} difference (20 nm) indicated that the stacking effect was enhanced after 365 nm UV-irradiation, and the enhancement of stacking was probably caused by the planar structure of MC which facilitates stacking formation. Overall, the spectroscopic study confirmed that intermolecular interactionsexisted among SPTPC molecules in the liposome bilayer membrane before and after UV exposure. The enhancement of MC-stacking after UV-irradiation could potentially perturb the bilayer structure and trigger the assembly-transition.

Thus, 365 nm UV irradiation switched SP to MC isomer, which perturbed the bilayer structure, and led to the collapse of liposome; cessation of UV light allowed a thermal-induced MC-to-SP recovery which removed the perturbation and caused re-formation of liposome. At molecular level, the collapse and re-formation of bilayer structure should involved a phase transition in bilayer membrane, relating with disorder and re-alignment of hydrocarbon chains of SPTPC. A polarized optical microscopy (POM) was applied to observe the assembly-transition, and to verify phase transition in bilayer membrane (Fig. 6a, 6b). In the bilayer membrane of SPTPC-liposomes, alignment of hydrocarbon chains forms a liquid crystalline phase and shows weak optical anisotropy or birefringence.[46, 47] Under POM with a 530 nm retardant plate, the birefringence results in yellow and blue interference colors of the liposome. Upon 365 nm UV-irradiation, the interference colors gradually faded away, which verifies the loss of birefringence and phase-transition of liquid crystalline into a disordered state in the membrane (Fig. 6a). Incomplete recovery of the interference colors was observed after the removal of UV-light (Fig. 6b). According to Michel-Levy color theory, the interference color of optically anisotropic materials depends on sample thickness, optical retardance, and effective birefringence.[46, 48] One explanation for the incomplete colour recovery is that the original liposomes before UV-irradiation had a multi-lamellar structure. Multi-layer membranes have larger optical anisotropy and exhibit obvious interference colors (yellow and blue), while the recovered liposomes might have uni-lamellar or oligo-lamellar structures, which exhibits smaller optical anisotropy and lighter interference colors. Thus, the change of interference colors of liposomes verified the perturbation of bilayer membrane and corresponding phase-transition during SP-MC switch cycle. Furthermore, the incomplete recovery of interference colors indicated that the MCs might not only induce intra-membrane interactions, but also inter-membrane interactions, which alter the lamellarity of the liposomes after one liposome-fiber switching cycle.

To characterize the liposome-to-fiber assembly-transition during 365 nm UV-irradiation, dynamic light scattering (DLS) was applied to the sonicated and extruded SPTPC-liposome. As Fig. 5d shows, the normalized correlation function curve after irradiation decayed more slowly than that before irradiation, which indicated slower diffusion rate of assembly after irradiation. The size distribution curve exhibited achange of polydispersity of the assembly (Fig. 5e). After 365 nm irradiation, the polydispersity increasedand a small peak emerged at high value of $\log_{10}$D indicating formation of an assembly with larger size. Though using size distribution to characterize fibrous assembly is not reasonable, the information from Fig. 5e about the fibrous assembly could be viewed as that of spherical particle that has the same translational diffusion coefficient. All of these changes of colloidal properties were explained by the assembly-transition from liposome to fibrous assembly, because the fiber has a larger size in one dimension and can form entanglements, which decrease the diffusion rate. 1-D WAXS curvesshowed that the intensity of the diffraction peak

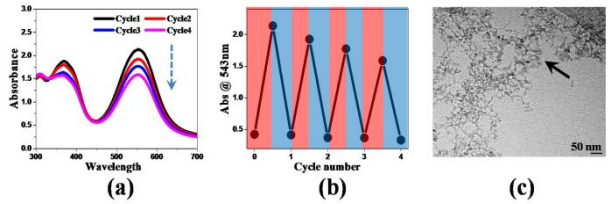

Fig. 7 (a) The UV-vis spectra of SPTPC-liposomes immediately after 365 nm UV-exposure in four irradiation/recovery cycles. (b) Absorption intensity changes (λ_{max}=543 nm) during four alternative irradiation/recovery cycles. Decrease of initial MC-absorption intensity indicates fatigue happens in each cycle. (c) Cryo-TEM image of SPTPC-liposomes sample after four irradiation/recovery cycles shows the presence of stacking aggregates (scale bar represents 50 nm).

had little change, from which nothing can be concluded. An increase of exposure time during WAXS measurements may give more appreciable results after UV-irradiation.

SP-fatigue induced by MC-stacking effect

The SPTPC-liposome system exhibits a unique, photo-inducible assembly-transition. Specifically, upon UV exposure, SP was switched to MC isomer, and MCTPCs trigger the emergence of additional molecular interaction. The SP-MC transition in each SPTPC building block enhances the influence of perturbations to liposomal structures, causing a drastic liposome-to-fiber transition. Unfortunately, the interactions of MCs generated fatigue of SP in each SP-MC switch cycle, which decreased the repeatability of photochromic characteristics and is disadvantageous for applications of this SP-based dynamic assembly. In the assembly-transition loop of SPTPC-liposomes, SP-fatigue occurred in each cycle of SP-MC transition (Fig. 7a, 7b). The fatigue induced a nearly 20% decrease of the initial intensity of MC-absorption band after four SP-MC switch cycles. To identify the reason for fatigue, ^{1}H NMR spectra were collected before and after the four SP-MC transition cycles, and the results suggest that there was no obvious decomposition of SP or MC (ESI, Fig S3). Thus, the fatigue was attributed to formation of stable MC-stacking aggregates. Stacking aggregation formed and inhibited recovery of MC to SP. Nanoscale aggregations in recovered samples were occasionally observed in cryo-TEM images (Fig. 7c black arrow).

Two-component liposomes (SPTPC/TPC): relief of MC-interaction and study of photo-responsiveness

A photo-inert triazole-phosphotidylcholines (TPC) was mixed with SPTPC to prepare two-component liposomes, aiming to dilute the percent of SPTPC in the bilayer membranes and relieve the SP-fatigue from MC-stacking (Fig. 8a). Liposome samples (1 mM) with different molar percentages of SPTPC were prepared using the hydration method in water (pH=7.04). The photo-induced morphological changes of these liposome samples were investigated by fluorescence microscopy, and

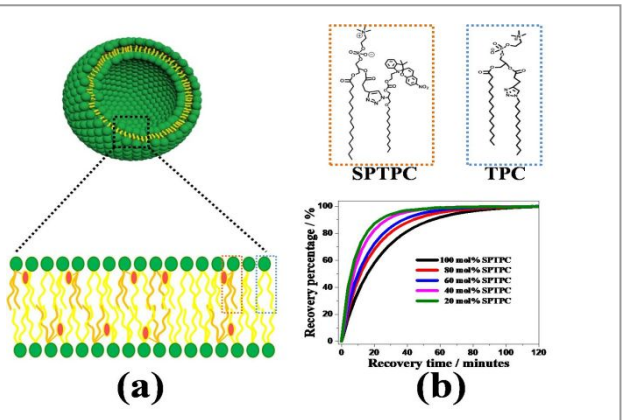

Fig. 8 (a) Schematic illustration of SPTPC/TPC two-component liposome prepared by the hydration method. (b) Recovery curve of MC-absorption band (intensity at 543 nm).

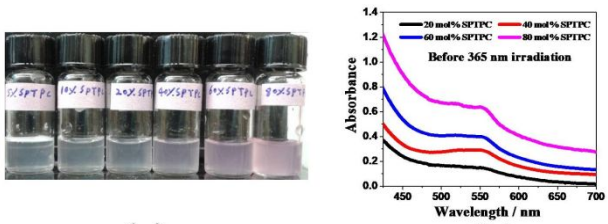

Fig. 9 (a) Appearance of SPTPC/TPC liposomes with different SPTPC% (after sonication and extrusion). Increased color indicates SP-to-MC switch (b) Absorption curves of SPTPC/TPC liposomes with different SPTPC%.

results showed that with decreasing SPTPC content, the degree of liposome photo-responsiveness was lower (ESI, movie S2-S3). Specifically, when the SPTPC content was less than 30 mol%, no obvious morphological changes were observed using fluorescence microscopy. For liposome samples with higher percentages of SPTPC (60~80 mol%), the morphological behaviour varied upon SPTPC-to-MCTPC photo-switching (ESI, movie S4-S6).

To investigate the effect of photo-inert TPC addition onthe thermally induced MC-to-SP switch, recovery of the MC absorption band was recorded (Fig. 8b). With higher percentages of TPC, MC-to-SP recovery was accelerated. Accelerated MC-to-SP recovery suggests that the addition of TPC in the bilayer membranes reduced molecular interactions around MC groups (e.g., MC-stacking effect), allowing the MC-to-SP isomerisation to process more quickly.

The SPTPC/TPC liposome (1 mM or 10 mM) dispersions were treated by sonication and extrusion (through 100 nm membrane). Before UV irradiation, increasing SPTPC content gradually led to appearance of a pink color, which indicated increased SP-to-MC isomerisation at higher SPTPC concentrations (Fig. 9a, 9b). DLS was used to characterize the effects of lipid concentration and UV irradiation on liposome size and polydispersity. For the 1 mM samples, increasing SPTPC content led to increased hydrodynamic diameter, but this trend was not observed for the 10 mM sample (Fig. 10a, 10b). The 10 mM liposome samples were also more polydisperse than 1 mM liposome samples (Fig. 10c, 10d and ESI Fig. S4), which is likely attributed to increased collisions between liposomes leading to additional inter-membrane interactions and potentially collision induced changes in assembly morphology.

The photo-responsiveness of the assemblies was also characterized by DLS. For 10 mM samples with SPTPC content equal to or greater than 60%, the hydrodynamic diameter was significantly different before and after 2 minutes of UV irradiation (15 mW/cm^2). This data supported that the photo-induced SP-to-MC transition triggered a morphological assembly response in the SPTPC/TPC liposomes with SPTPC content above 60% (Fig. 10a, 10b). The same photo-responsiveness, however, was not observed for 1 mM liposomes, suggesting a total-PC-concentration dependent photo-responsiveness, which provides further evidence that

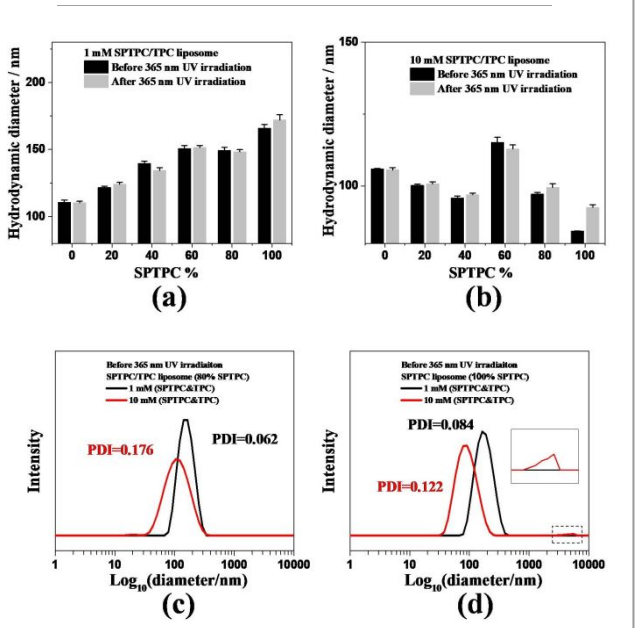

Fig. 10 (a) At 1mM total-PC concentration, hydrodynamic diameter change of SPTPC/TPC liposome (different SPTPC%) before and after 365 nm UV irradiation. (b)At 10mM total-PC concentration, hydrodynamic diameter change of SPTPC/TPC liposome (different SPTPC%) before and after 365 nm UV irradiation. (c) Before 365 nm UV irradiation, comparison of size distribution curve of SPTPC/TPC liposome (80% SPTPC) with different total-PC concentration (1 mM and 10 mM). (d) Before 365 nm UV irradiation, comparison of size distribution curve of SPTPC liposome (100% SPTPC) with different total-PC concentration (1 mM and 10 mM).

inter-membrane interactions play a role in photo-induced morphology changes. At higher phospholipid concentrations, more liposomes were present and increased collision events and membrane-contacting. Upon irradiation, the presence of more MC functionalities near the hydrophilic liposomal surface likely strengthened the inter-membrane interactions due to the MC stacking effect, and led to more apparent morphological changes of the liposomes. The above results combined with initial studies of SPTPC assembly and photo-induced assembly-transition supported thatthe inter-membrane MC-stacking was the driving force of photo-induced assembly-transitions.

The effect of other intrinsic properties of the MC groups, such as zwitterionic structure, dipolar moment, and hydrophilicity, on the assembly-transition should not be neglected. A possible effect from those MC properties is to increase phase mobility of the bilayer membrane by phase transition of the aliphatic chains (Fig. 6). To verify that the phase transition increases phase mobility in the bilayer membrane of SPTPC/TPC liposome, a photo-patterning method was used to achieve selective irradiation of the samples. Fig. 11 shows the morphological evolution of a 70 mol% SPTPC/TPC-liposome sample upon partial exposure to 370 nm light. A tubular liposome first underwent a tubular-to-spherical shape-transition, subsequently several bright patches appeared on the surface of

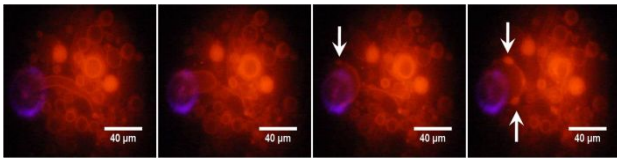

Fig. 11 Selective irradiation of SPTPC/TPC liposomes (70 mol% SPTPC) and the photo-induced two-step morphological change: tubular to spherical shape, and formation of MCTPC-rich phases (white arrows). Scale bars represent 20 microns.

the spherical liposome. The patches moved and expanded with prolonged irradiation time (Fig. 11, white arrows). In the tubular-to-spherical transition step, SPTPCs in the irradiation area were switched to MCTPC and phase transition was triggered in this area of the bilayer membrane. The un-switched SPTPCs and photo-inert TPCs maintained bilayer membrane integrity and prohibited the assembly transition into fibers. Thus, the tubular liposome adjusted the contour from tube to sphere to lower the free energy of the entire system. The tubular-to-spherical transition indicated increased phase-mobility in the bilayer membrane. In the second step, the bright patches were MCTPC-rich phases in bilayer membrane. The intrinsic fluorescence excitation and emission bands of MCTPC overlap with the filter set-up of the microscope, so fluorescence of MCTPC-rich phases appeared brighter. The translocation of the MCTPC-rich phases can also be ascribed to the increased phase mobility in the bilayer membrane, which was likely induced by perturbation from MCs and MC-stacking. Un-switched SPTPCs and MCTPC-rich phases moved into and out of the selected irradiation area, respectively, resulting in MCTPC enrichment and formation ofnew MCTPC-rich phases.

Conclusion

In summary, a spiropyran-containing triazole-phosphotidylcholine (SPTPC) was synthesized by a CuAAC reaction. The PC moiety enabled SPTPC to self-assemble in water. Due to special position of SP in SPTPC structure, a small portion of SP was switched to MC by exposure to polar microenvironments (i.e., water). The MC groups increased inter-membrane interactions, specifically MC-stacking, which influenced the morphology of SPTPC assembly, and resulted in co-existence of liposomes and fibers. Upon 365 nm UV irradiation, the SP-to-MC switch strengthened the inter-membrane MC-stacking, and led to liposome-to-fiber assembly transition. Though a thermal-induced MC-to-SP recovery resulted in re-formation of liposomes, MC-stacking caused undesirable fatigue during SP-MC switch cycles. By addition of photo-inert TPC molecule, a two-component SPTPC/TPC liposome was obtained. SPTPC content of SPTPC/TPC liposomes influenced inter-membrane MC-interactions and, in turn, the photo-responsiveness of SPTPC containing liposomes. The phospholipid-characteristic and reversible liposome-to-fiber assembly-transition make SPTPC a promising candidate for

adaptive assembly applications, such as constructing stimuli-responsive organelles in artificial cells.

Conflicts of interest

There are no conflicts to declare.

Acknowledgements

This work was supported by the U.S. Army Research Office (MURI program, Award W911NF-13-1-0383). The authors gratefully acknowledge use of WAXS facilities and instrumentation supported by NSF MRSEC Grant DMR-1420736. The electron microscopy was done at the University of Colorado, Boulder EM Service Core Facility in the Dept. of MCD Biology, with the technical assistance of facility staff. The fluorescent imaging work was performed at the BioFrontiers Institute Advanced Light Microscopy Core at the University of Colorado Boulder. We thank Megan Mitchell for preparation of uni-lamellar liposomes using tip-sonicator and membrane extruder, Dr. Joseph Dragavon for assistance in fluorescence microscopy, and Dr. Shen Hao for assistance in photo-patterning setup.

Notes and references

1. Q.-D. Hu, G.-P. Tang and P. K. Chu, *Accounts Chem. Res.*, 2014, **47**, 2017-2025.
2. V. Allain, C. Bourgaux and P. Couvreur, *Nucleic acids Res.*, 2011, **40**, 1891-1903.
3. L. Schoonen and J. van Hest, *Adv. Mater.*, 2016, **28**, 1109-1128.
4. A. Das and S. Ghosh, *Angew. Chem. Int. Ed.*, 2014, **53**, 2038-2054.
5. M. Moazeni, F. Karimzadeh and A. Kermanpur, *Soft Matter*, 2018.
6. M. Antonietti and S. Förster, *Adv. Mater.*, 2003, **15**, 1323-1333.
7. A. Wang, W. Shi, J. Huang and Y. Yan, *Soft Matter*, 2016, **12**, 337-357.
8. C. T. Ambrose, *Cell. Immunol.*, 2006, **240**, 1-4.
9. O. Kedem and A. Katchalsky, *Biochim. Biophys. Acta*, 1958, **27**, 229-246.
10. D. Philp and J. F. Stoddart, *Angew. Chem. Int. Ed.*, 1996, **35**, 1154-1196.
11. M. Edidin, *Annu. Rev. Bioph. Biom.*, 2003, **32**, 257-283.
12. D. Brown and E. London, *Annu. Rev. Cell. Dev. Bi.*, 1998, **14**, 111-136.
13. H. T. McMahon and J. L. Gallop, *Nature*, 2005, **438**, 590.
14. B. Li, Y.-P. Cao, X.-Q. Feng and H. Gao, *Soft Matter*, 2012, **8**, 5728-5745.
15. C. Chassenieux and C. Tsitsilianis, *Soft Matter*, 2016, **12**, 1344-1359.
16. A. Nuthanakanti and S. G. Srivatsan, *Nanoscale*, 2016, **8**, 3607-3619.
17. X. Wang, J. Hu, G. Liu, J. Tian, H. Wang, M. Gong and S. Liu, *J. Am. Chem. Soc.*, 2015, **137**, 15262-15275.
18. C. Li, Y. Zhang, J. Hu, J. Cheng and S. Liu, *Angewandte Chemie*, 2010, **122**, 5246-5250.
19. J. Yuan, S. M. Hira, G. F. Strouse and L. S. Hirst, *J. Am. Chem. Soc.*, 2008, **130**, 2067-2072.
20. X. Li, X. Ma, D. Fan and C. Zhu, *Soft Matter*, 2012, **8**, 3781-3790.
21. C. Yan, A. Altunbas, T. Yucel, R. P. Nagarkar, J. P. Schneider and D. J. Pochan, *Soft Matter*, 2010, **6**, 5143-5156.
22. E. R. Gillies, T. B. Jonsson and J. M. Fréchet, *J. Am. Chem. Soc.*, 2004, **126**, 11936-11943.
23. Y. Bae, S. Fukushima, A. Harada and K. Kataoka, *Angew. Chem. Int. Ed.*, 2003, **42**, 4640-4643.
24. R. De La Rica, D. Aili and M. M. Stevens, *Adv. Drug Del. Rev.*, 2012, **64**, 967-978.
25. C. Li and S. Liu, *Chem. Commun.*, 2012, **48**, 3262-3278.
26. K. S. Moon, H. J. Kim, E. Lee and M. Lee, *Angew. Chem. Int. Ed.*, 2007, **46**, 6807-6810.
27. H. M. Zareie, C. Boyer, V. Bulmus, E. Nateghi and T. P. Davis, *Acs Nano*, 2008, **2**, 757-765.
28. B. C. Buddingh' and J. C. van Hest, *Accounts Chem. Res.*, 2017, **50**, 769-777.
29. T. Hamada, Y. Miura, K.-i. Ishii, S. Araki, K. Yoshikawa, M. d. Vestergaard and M. Takagi, *J. Phys. Chem. B*, 2007, **111**, 10853-10857.
30. O. Wesolowska, K. Michalak, J. Maniewska and A. B. Hendrich, *Acta Biochim. Pol.*, 2009, **56**, 33.
31. Y. Wu, T. Sasaki, K. Kazushi, T. Seo and K. Sakurai, *J. Phys. Chem. B*, 2008, **112**, 7530-7536.
32. W. Tian and J. Tian, *Dyes Pigments*, 2014, **105**, 66-74.
33. S. Swansburg, E. Buncel and R. P. Lemieux, *J. Am. Chem. Soc.*, 2000, **122**, 6594-6600.
34. K. H. Fries, J. D. Driskell, S. Samanta and J. Locklin, *Analytical Chemistry*, 2010, **82**, 3306-3314.
35. M. Natali and S. Giordani, *Organic & biomolecular chemistry*, 2012, **10**, 1162-1171.
36. J. Fonollosa, L. Campos, M. Martí, A. de la Maza, J. L. Parra and L. Coderch, *Chem. Phys. Lipids*, 2004, **130**, 159-166.
37. D. Zhang, Q. Liu, R. Visvanathan, M. R. Tuchband, G. H. Sheetah, B. D. Fairbanks, N. A. Clark, I. I. Smalyukh and C. N. Bowman, *Soft Matter*, 2018, **14**, 7045-7051.
38. T. McIntosh, M. Stewart and D. Downing, *Biochemistry*, 1996, **35**, 3649-3653.
39. M. Wilkins, A. Blaurock and D. Engelman, *Nature New Biology*, 1971, **230**, 72-76.
40. R. Klajn, *Chemical Society Reviews*, 2014, **43**, 148-184.
41. D. Papahadjopoulos and N. Miller, *Biochimica et Biophysica Acta (BBA)-Biomembranes*, 1967, **135**, 624-638.
42. R. Heiligman-Rim, Y. Hirshberg and E. Fischer, *J. Phys. Chem.*, 1962, **66**, 2465-2470.
43. L. Angiolini, T. Benelli, E. Bicciocchi, L. Giorgini and F. M. Raymo, *React. Funct. Polym.*, 2012, **72**, 469-477.
44. L. Angiolini, T. Benelli, L. Giorgini and F. M. Raymo, *Macromol. Chem. Phys.*, 2008, **209**, 2049-2060.
45. W. Miao, S. Wang and M. Liu, *Adv. Funct. Mater.*, 2017, **27**.
46. S. Bibi, R. Kaur, M. Henriksen-Lacey, S. E. McNeil, J. Wilkhu, E. Lattmann, D. Christensen, A. R. Mohammed and Y. Perrie, *Int. J. Pharmaceut.*, 2011, **417**, 138-150.
47. D. Zhang, Z. Liu, D. Konetski, C. Wang, B. T. Worrell and C. N. Bowman, *Rsc Adv.*, 2018, **8**, 14669-14675.
48. D. S. Miller, R. J. Carlton, P. C. Mushenheim and N. L. Abbott, *Langmuir*, 2013, **29**, 3154-3169.